IEEE Access
Multidisciplinary | Rapid Review | Open Access Journal

Received 14 July 2022, accepted 21 September 2022, date of publication 30 September 2022, date of current version 5 October 2022.

Digital Object Identifier 10.1109/ACCESS.2022.3211099

RESEARCH ARTICLE

Design and Analysis of GO Coated High Sensitive Tunable SPR Sensor for OATR Spectroscopic Biosensing Applications

MD. AREFIN ISLAM[1], (Student Member, IEEE), ALOK KUMAR PAUL[1], (Member, IEEE), BELAL HOSSAIN[1], (Member, IEEE), AJAY KRISHNO SARKAR[1], (Member, IEEE), MD. MAHABUBUR RAHMAN[2], ABU SADAT MD. SAYEM[3], ROY B. V. B. SIMORANGKIR[4], (Member, IEEE), MD ASADUZZAMAN SHOBUG[5], (Graduate Student Member, IEEE), JOHN L. BUCKLEY[4], (Member, IEEE), KISALAYA CHAKRABARTI[6], (Senior Member, IEEE), AND ALI LALBAKHSH[3,7], (Senior Member, IEEE)

[1]Department of Electrical and Electronic Engineering, Rajshahi University of Engineering and Technology, Kazla, Rajshahi 6204, Bangladesh
[2]Department of Electrical and Computer Engineering, Rajshahi University of Engineering and Technology, Kazla, Rajshahi 6204, Bangladesh
[3]School of Engineering, Macquarie University, Sydney, NSW 2119, Australia
[4]Tyndall National Institute, University College Cork, Cork, T12R5CP Ireland
[5]Department of Electrical and Electronic Engineering, Pabna University of Science and Technology, Pabna 6600, Bangladesh
[6]Electronics and Communication Engineering, Haldia Institute of Technology, Haldia, West Bengal 721657, India
[7]School of Electrical and Data Engineering, University of Technology Sydney (UTS), Sydney, NSW 2007, Australia

Corresponding authors: Roy B. V. B. Simorangkir (roy.simorangkir@tyndall.ie) and Ali Lalbakhsh (ali.lalbakhsh@mq.edu.au)

ABSTRACT In this paper, we numerically debrief an ultra-high sensitive surface plasmon resonance (SPR) biosensor utilizing thin layers of graphene oxide (GO) that have not been addressed adequately till now. By the deposition of GO on top of the metal-dielectric heterostructure, our proposed sensor can achieve higher sensitivity and higher Quality Factor (QF) simultaneously which has not been possible by the existing models to our knowledge. Because of its large surface area and sp^2 inside of an sp^3 matrix which is capable of confining π electrons, GO can form strong covalent bonds with biomolecules and hence enhanced light-material interaction that made researchers contemplate to achieve increased sensitivity and figure of merit. Both the transfer matrix method and finite element method are exploited to perform extensive numerical analysis for optimizing the structure considering its sensitivity, full width half maximum (FWHM), and QF. This paper examines six different configurations of multilayer heterostructure containing prism-adhesive-metal-$BaTiO_3$/BP-Gr/GO/MXene-sensing medium, and a noticeably enhanced performance is achieved using GO with a maximum sensitivity of 372 deg/RIU and QF of 88.11 RIU^{-1} in the range of refractive index (RI) 1.330 to 1.353. Moreover, the possibility of designing a tunable SPR sensor to operate at a broader range of analyte's RI is investigated, and 414 deg/RIU with 119.27 RIU^{-1} QF at 1.407 RI is achieved. The Electric field distribution, effects of different layers, and fabrication feasibility of the proposed sensor are explored, it is envisaged that this can be an appropriate apparatus for highly sensitive, rapid, and noninvasive label-free biosensing useful in experimental sensing protocols.

INDEX TERMS Composite layer sensor, figure of merit, graphene oxide, MXene, surface plasmon resonance, two-dimensional materials.

I. INTRODUCTION

The brisk growing advancement of engineering design and technology has glorified us with highly sensitive biomedical equipment capable of identifying various diseases and biomolecules. Optical biosensors are the newest wing in this realm because of the changes in optical parameters concerning the surrounding environment allowing fast and accurate detection [1]. Regarding practical sensing applications, surface plasmon resonance technology has piqued the

The associate editor coordinating the review of this manuscript and approving it for publication was Chao Zuo.

interest of numerous scientist groups and leading the way of optical sensing owing to its significant advantages over conventional biosensors, which include higher sensitivity, simplicity of use, and lower cost, real-time rapid label-free detection [2]. It has a wide range of applications in the biosensing industry, including detection, analysis, and characterization of biomolecules, chemicals, environmental protection, human blood group, glucose, bacteria, living cell analysis, DNA hybridization, water, and food safety, etc., which have a direct bearing on human health [3], [4], [5], [6], [7]. Biosensors based on this technology are still on the play for early detection of new emerging viruses like SARS-CoV-2 [8]. In recent years, carbon nanotube field effect-based biosensors have gained popularity for their unique features like low cost, real-time, and ultrasensitive detection of tiny biomolecules. Semiconducting carbon nanotubes (sc-CNTs) are auspicious for FET channel integration that can replace Si based technology allowing better and more accurate detection of life-threatening infectious diseases [9]. Using Y-Function Method (YFM) equation, Alabsi *et al.* mathematically investigated the effect of variation of certain physical parameters on electronic features improving the CNTFET devices sensing performance [10]. The fundamental operating mechanism of SPR biosensors is to analyze variations in input incoming light and determine the changes in its characteristics at the output terminal, specifically, the fluctuation in frequency, amplitude, phase, wavelength, or polarization of light [11]. These sensors bypass the time-consuming labeling process for molecule binding and offer real-time monitoring, label-free detection, and analysis of the analytes. Surface plasmon polaritons (SPP), the propagating electromagnetic (EM) waves through the metal-dielectric interface, are sensitive to very small changes in the RI (10^{-7} order) of the analyte [12]. The plasmon is classified into three types, namely surface plasmon, bulk plasmon, and localized surface plasmon. This work focuses on a sensor based on the first type, which is formed at metal-dielectric interlace and activated by EM radiation [12], [13]. For SPR to occur, two criteria are needed, the incident light to be p-polarized or a Transverse Magnetic (TM) wave, and the evanescent waves (EW) produced by optical attenuated total reflection (OATR) at the prism-metal interface must be matched with the surface plasmon wave vectors (SPWV) [14], [15]. The SPR detects biomolecular interactions in a small axial area on the sensor surface, which in turn forms a sensing field when incoming light on the sensor surface excites the SPs. At the resonance frequency, for which the previously mentioned two criteria meet, a sharp dip of reflected light intensity is obtained for the particular RI of the analyte which is referred to as the reflectivity curve. In this situation, the whole reflectivity curve can be plotted in the angular reflection spectrum as a result of energy dissipation into the metallic layer or scattering on the sensor surface. With its greater shift angle and simple production procedure, this kind of sensor is more preferable and suitable for instant detection with higher sensitivity than other optical detection techniques such as Ramman Scattering [13], fiber Bragg grating (FBG) [5], planner waveguide [16], or optical fiber sensor [17].

The Kretschmann prism coupling is the best for modeling the arrangement where it comprises a prism of low RI like BK7, CaF_2, or SF10 and a thin coating of metal such as gold (Au), copper (Cu), silver (Ag), aluminum (Al), etc. The dielectric constant of metal is the prime determinant to picking the suitable metal to design the sensor where in between Au and Ag, the two most common metals for these types of configurations, the latter one can generate a narrower and more acute SPR curve due to its small optical damping, and sharper resonance peak with little to no inter-band transmission at the visible region [7]. In contrast, the Au layer's low molecule binding capacity restricts the Au-based SPR sensor's performance. High sensitivity is attained using Ag as the plasmonic metal in [18], and Han *et al.* evaluated the influence of different materials on performance, revealing that structures with Ag have a significantly more outstanding performance [19]. With a high work function of 4.74 eV, Ag can transmit a huge amount of electrons leading to electric field enhancement at the sensing interface and hence improving sensing and detection accuracy. Despite its chemical inertness and no inter-band transfer at the visible light frequency, Ag is highly prone to oxidation which may degrade the device's performance and usability over time. For the sake of developing a more realistic model, an appropriate adhesive layer with little to no influence on performance is required to overcome the limitations to improve the overall stability and performance of the proposed construction. Chromium (Cr) and titanium (Ti) are often utilized as adhering layers during thin film deposition (e.g. in evaporation techniques) as these materials all have well characteristics needed to attach with typical substrate materials [20]. They have a vigorous oxygen-binding strength and so may de-passivate many materials surfaces. In such cases, oxygen atoms might act as a bridge between the substrate and the coating [21]. Though Ti is softer than Cr, a thin covering of any of them would have minimal impact on device performance but greatly improve device stability [22].

Since Biacore introduced prism-coupled sensors to the market in 1990, academics, analysts, and researchers are always trying to enhance its performance. According to recent research, combining dielectric material with metal dramatically improves the device's sensitivity and other parameters [27], [31]. SPPs are formed on the upper and lower interfaces of the metal and dielectric layer when p-polarized light is incident along with the metal and dielectric surface. The dielectric constants of the two dielectrics (say ε_1, and ε_2) should satisfy the condition [32] which effectively causes the stimulation of two SPs modes on the opposite side of the contact. It is mainly due to the fact that the effective refractive index of the single SPW splits into two bound eigenmodes which are demonstrated in [33] and [34]. These two eigenmodes have symmetric and antisymmetric bound magnetic field properties. One is long-range surface plasmon (LRSP), which has a symmetric field profile, whereas the

TABLE 1. Summarizing performance due to various materials and their modeling studies.

Material Consideration	SPR Sensor Structure	Numerical and Modeling Studies	Sensitivity [deg/RIU]	QF [1/deg]	Ref
Ag	Bk7-Ag-Si-Franckeite	TMM and FEM	158.31	63.92	[7]
	Bk7-Ag-SnSe-BlueP/MoS_2	TMM and FEM	168	20.97	[23]
$BaTiO_3$	Bk7-Ag-$BaTiO_3$-Graphene	TMM	257	45.05	[24]
BP	Bk7-Au-WSe2-PtSe2-BP	TMM and FEM	200	17.70	[25]
	Bk7-Au-BP-Au-Graphene	TMM and FEM	218	26.13	[26]
Graphene	Bk7-ZnO-Ag-$BaTiO_3$-Gr	TMM	168	58.33	[27]
	Bk7-Ag-Graphene-Au-WS_1/MoS_2	TMM	203	28.31	[28]
Graphene Oxide	Bk7-Au-GO	TMM	151.87	33.38	[29]
MXene	CaF_2-Ag-Bp-$Ti_3C_2T_x$ (MXene)	TMM	322	55.596	[30]

other, known as short-range surface plasmon (SRSP), has an anti-symmetric field profile. The symmetric field profile of the LRSP mode demonstrates energy confinement at the metal-dielectric contact, hence, higher sensitivity than conventional SPR sensor [32], [33], [35]. Among the previously reported works using dielectric materials [19], [33], [36], Barium titanate ($BaTiO_3$) has exceptional dielectric characteristics, including a high RI, and low dielectric losses. It has a porosity of 50–70% with an average pore diameter of 30 μm. It is also reported that the shape of tetragonal crystalline $BaTiO_3$ nanoparticles does not change over time [24]. Sun *et al.* [24] have used $BaTiO_3$ layer with thick Ag and achieved 257 deg/RIU sensitivity with Quality Factor (QF) of 45.05 RIU^{-1}. Parallel to this, the research community is looking for new potential materials to increase sensor performance, and they've come up with two-dimensional nanomaterial that has enhanced sensor performance because of its unprecedented optical, catalytic, and electronic features. Several 2D materials have been proposed in the past decade due to their remarkable physicochemical merits onto targeted molecules, configurable bandgap, adsorption energy features, and suitable physical attributes [37], [38], [39]. Graphene (Gr) for example, the most popular 2D material for the past years [4], [6], [19], [24], [27], [31], has tremendous mechanical and electrical facets. It has a low S/N ratio and good target analyte responsiveness. A monoatomic layer of graphene has sp^2 hybridized carbon atoms in a 2D honeycomb lattice structure, so the enormous surface area and robust stacking with hexagonal cells reveal the graphene layer's great absorption capabilities [12]. Han *et al.* [19] has got 216.8 deg/RIU and Kumar *et al.* [27] reported 58.33 RIU^{-1} QF with a sensitivity of 168 deg/RIU using Gr as the top layer. Graphene has also been used with other 2D materials like WS_2-MoS_2 in [40] and [28]. For future optoelectronic sensing devices, phosphorene has recently gained a lot of attention in the scientific community, the most important phosphorus allotrope is black phosphorus (BP) which has different atomic ledges stacked together by Van der Waals interactions. Bulk BP is a hylic element having a graphite-like structure that can be mechanically exfoliated into an ultra-thin nanosheet other than graphite. It is a p-type semiconducting material with a direct bandgap of 0.3 eV and field-effect mobility depends on the layer thickness [41], [42]. In theoretical investigations, it is found that BlueP is more stable than BP and has an adjustable bandgap that ranges from 2 to 1.2 eV from monolayer to bulk [43], [44]. Wu *et al.* [42] have achieved maximum angular sensitivity of 279 deg/RIU using BP with bilayer WSe_2 while 200 deg/RIU sensitivity with 17.70 RIU^{-1} of quality factor is achieved in [25]. Han *et al.* [31] have reported maximum sensitivity of 348.8 deg/RIU using BlueP with a monolayer of Graphene and has also been used along with SnSe for cancerous cell detection in [23].

GO has garnered significant interest in recent years in the domains of plasmonic and SPR biosensors as a novel class of two-dimensional carbon nanostructures from both practical and theoretical scientific findings. GO offer exceptional optical and biosensing capabilities having a large surface area and sp^2 inside a sp^3 matrix which can confine π-electrons and improve molecule adsorption [45], [46]. The direct bandgap behavior of GO may be regulated by oxidation, which produces photoluminescence and makes chemically functionalized GO that results in biological applications. In direct bandgap material, the k-vector (crystal momentum) of the electrons and holes in both the conduction band and valence band is the same. Direct bandgap material tends to have a lower effective mass of electrons and lets electrons travel faster comparatively. This leads to a greater possibility of occurring strong surface plasmon resonance in that region. For this reason, GO is a perfect material to be used in photoluminescence applications as emitting photons will be easier from them instead of any indirect bandgap material and we are capable of controlling it by changing oxidation. Moreover, as a strong resonance field can be generated by GO, they are chemically functionalized and one of the ideal elements to be used in biological applications based on of surface plasmon resonance (SPR) phenomena. To improve surface area sensing, the carboxyl groups of a GO film may be transformed into amine-reactive groups. Furthermore, by altering the oxygen-containing functional groups on the surface of GO, the bandgap and dielectric constant may be increased, hence increasing the SPR characteristics [47], [48]. Nurrohman and Chiu [29] have investigated the effect of using the GO layer, revealing that GO has increased the Figure of Merit (FOM) of their proposed SPR sensor to 33.41 RIU^{-1} with a sensitivity of 151.87 deg/RIU in comparison with Graphene on the same structure. MXene ($Ti_3C_2T_x$), another

prosperous 2D material, has recently shown potential for biochemical and biomolecular sensing when utilized as an interaction layer in SPR. Its distinctive qualities include increased hydrophilic surface area, strong carrier confinement, chemical, and mechanical stability, reduced work function, layered nature, and higher binding energies for biomolecules [49]. Pandey [30] have reported 322 deg/RIU sensitivity and 55.596 RIU^{-1} FOM using 3 layers of MXene-BP while Wu *et al.* [50] have achieved 225.4 deg/RIU sensitivity at 532 nm wavelength. Performance of these existing models in terms of various materials is summarized in Table 1 which compares their achieved Sensitivity and QF as well as the numerical and modeling studies they have implemented.

While other reported works strive for high sensitivity or high QF out of their proposed model, the novelty of this work is it presents and investigated a state of the art high-performance SPR sensor by employing graphene oxide on top of the prism-adhesive-metal-dielectric structure that can achieve both ultra-high sensitivity and good QF simultaneously. The sensing performance of the proposed structure is determined by characterizing the sensor's reflectivity curve. Numerical modeling to simulate findings for the suggested SPR sensor for commercial-scale prototyping has been carried out analytically. Although the entire study was based on simulation work and theoretical calculations, we have justified our methodology by simulating the single silver layer configuration in [51]. The outcome of the simulation nearly aligned with the experimental findings with a deviation of 0.10 degree for water and 9.78 degree for Acetone as analyte which proves the relevancy of the simulation work.

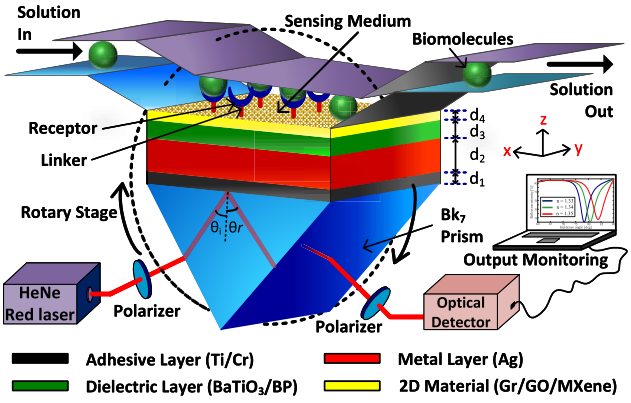

FIGURE 1. Schematic diagram of the proposed SPR sensor based on Otto-Kretschmann configuration.

The proposed model has achieved 372 deg/RIU sensitivity and 88.11 RIU^{-1} QF, moreover the authors have further demonstrated the possibility of making a tunable SPR sensor to achieve higher sensitivity at a higher range of RI. Achieving high performance parameters concurrently has not been possible until now that will be reflected by the comparison table at the end of the article. In section II, we will go through the interpretation of different layers used to build the sensor, mathematical equations for reflectivity, and performance evaluating parameters. In section III, we will investigate the performance of the six configurations from different aspects, effect on parameters by the variation of all layer thickness, and using different type of dielectric and 2D materials. We will also demonstrate the possibility of tuning the sensor to achieve better performance at higher RI and analysis of Electromagnetic field distribution will be carried out in this section.

II. THEORETICAL MODELING AND DESIGN ANALYSIS

A. INTERPRETATION OF CONSTITUENT LAYERS

Fig. 1 implies the proposed structure of the SPR biosensor using a glass prism and layers of materials in the Otto-Kretschmann configuration. This configuration can enhance surface field strength thereby a dip in the reflectance curve can be achieved for the waveguide coupled long range SPR sensor. To achieve the maximum excitation of the surface plasmon on the structure, we examined the effect of different types of adhesive layers (Cr and Ti), dielectric material ($BaTiO_3$ and BP), and 2D material (Graphene, GO, and MXene). Also, thickness of the layers d_1, d_2, d_3, and d_4 are varied and their effect on performance are evaluated in the following sections. CaF_2, Bk7, Fk51A, SF10 prism can be chosen, whereas, in this model, the Bk7 prism is used to couple TM polarized optical monochromic light of λ = 632.8 nm wavelength. The low RI of the BK7 prism makes it an appropriate supplementary material for wave vector matching and hence high sensitivity. Maximum excitation of SPP occurs at the visible region (λ = 400 nm to 633 nm) thereby Helium-Neon red laser is used which provides a Gaussian beam shape along with less divergence. The RI of the prism can be calculated by,

$$n^2_{Bk7}(\lambda) = 1 + \frac{B_1\lambda^2}{\lambda^2 - C_1} + \frac{B_2\lambda^2}{\lambda^2 - C_2} + \frac{B_3\lambda^2}{\lambda^2 - C_3} \quad (1)$$

Taking λ in the micrometer unit, Equation (1) is valid from the 300 to 2500 range whereas the coefficients are taken from [24]. Metals have traditionally been employed as a key source for SPs creation in SPR sensors owing to their abundance of free electrons. The prism surface is coated with a thin Ag film of thickness d_2 as the noble metal for exciting SPP with adhesive sandwiched in between them. The Drude formula is used to express the complex dielectric function of any metal layer as,

$$\varepsilon_m(\lambda) = \varepsilon_{re} + i\varepsilon_{im} = 1 - \lambda^2\gamma_c / \left[\gamma_p^2(\gamma_c + i\lambda)\right] \quad (2)$$

Here, γ_p is the plasma wavelength analogous to the bulk plasma frequency, and γ_c is the collision wavelength which can be found for Ag in [42]. The RI of the material can be found by calculating the square root of this complex function. To adequately adhere the metal film to the glass substrate, a very thin layer of adhesive with thickness d_1 is deposited which inherently shields the Ag from oxidation. As adhesive material, the RI of both Ti and Cr are taken from measurement data in [52]. With thickness $d_3 = L * t_L$,

$BaTiO_3$ is grown on the metal surface for the config. *i-iii* with monolayer thickness of $t_L = 1\,nm$. BP is used for the config. *iv-vi* having $t_L = 0.53\,nm$, where L is the number of layers used. RI of the dielectric material is frequency-dependent and for the operating λ, it is $n_{BaTiO_3} = 2.4043$ that can be obtained from experimental data in [53], Mao *et al.* has reported RI of BP at the visible region in [54].

Finally, Gr (config. *i, iv*), GO (config. *ii, v*), or MXene (config. *iii, vi*) nanosheet is deposited over the structure which thickness is taken as $d_4 = M * t_M$, where M is the number of layers. Monolayer thickness of graphene is $t_M = 0.34\,nm$, and RI can be calculated using $n_{Gr} = 3.0 + i\,(C_1/3\,)\,\lambda$ where C_1 can be found in [29]. The RI of GO, a novel 2D material, depends on the monolayer thickness, $t_M = 2.55\,nm$ of the sheet and can be calculated using the formula, $n_{GO} = \sqrt{\varepsilon_{re} + i\varepsilon_{im}}$. Here, dielectric constants of this film can be found from experimental data which is $\varepsilon_{re} = 1.62$ and $\varepsilon_{im} = 0.01$ for this particular thickness [55]. Table 2 summarizes all the six configurations and their layer's thicknesses.

TABLE 2. All six configurations and their layer's thickness.

Configuration	SPR Sensor Structure	d_3	d_4
i	Bk7-Cr-Ag-$BaTiO_3$-Graphene-Analyte	L*1 nm	M*0.34 nm
ii	Bk7-Cr-Ag-$BaTiO_3$-GO-Analyte	L*1 nm	M*2.55 nm
iii	Bk7-Cr-Ag-$BaTiO_3$-MXene-Analyte	L*1 nm	M*0.993 nm
iv	Bk7-Cr-Ag-BP-Graphene-Analyte	L*0.53 nm	M*0.34 nm
v	Bk7-Cr-Ag-BP-GO-Analyte	L*0.53 nm	M*2.55 nm
vi	Bk7-Cr-Ag-BP-MXene-Analyte	L*0.53 nm	M*0.993 nm

The π conjugation structure of the GO layer, acting as a biomolecular recognition element, greatly increases macromolecular capture and so as a consequence, even small changes in the sensing medium's RI (n_s) may cause huge shifts in the SPR curve improving sensitivity and detection accuracy [38]. RI of the sensing medium is taken as $n_s = 1.330 + \delta_n$, where δ_n represents the change in RI owing to biological molecule absorption on the sensing layer surface. The SPR phenomenon is activated by altering the incidence angle of the incoming monochromatic polarized light beam. Evanescent wave vector (EWV) that enters in the metal layer, creates surface plasmon if it matches the wave vector (WV) at a certain angle termed as resonance angle, θ_{res}. This resonance angle fluctuates with sample solution concentration allowing for detection of the biomolecular component presence and its density as well. The whole setup is mounted on a rotatable platform as depicted in Fig. 1, a photodetector on the opposite side of the prism will detect minimum light reflection which is referred to as minimum reflectance, $R_{\min}$.

The possibility of practical implementation of the proposed sensor highly depends on the fabrication feasibility of the structure. To deposit the thin Ag layer, popular methods like vacuum thermal coating procedure, activated reactive type physical vapor deposition (ARE-PVD), or wet chemistry deposition method can be followed after performing some mandatory chemical pre-processing. The ion plating sputtering technique can be implemented to uniformly deposit the thin adhesion layer on the prism surface. This technique is one of the most advanced surface finishing process which makes the surface more durable with excellent adhesion power to the coating. However, uniform nanolayer coating with high efficiency and little surface roughness can be achieved by CVD [20]. Smith *et al.* [48] propose various low-cost easier techniques like spin coating, wet-spinning, and vacuum spinning methods to deposit the GO layer by which nanofilm of the material can be fabricated.

B. MATHEMATICAL EQUATIONS FOR REFLECTIVITY

Detailed numerical analysis was carried out by the N-layer Transfer Matrix Method (TMM) and later simulated with the help of the Finite Element Method (FEM) to achieve the reflectivity curve of the proposed sensor at the optimal thickness. Results are pretty accurate in the first case as the TMM method doesn't require any approximation. Stacking all the layers vertically along with the z-axis, the Fresnel equation with proper boundary condition gives reflection intensities, at various angles which can be expressed as $R_p = r_p r_p^* = |r_p|^2$ [23]. For N-layer, M_{ij} is the characteristics matrix denoted as,

$$M_{ij} = \left(\prod_{k=2}^{N-1} M_k\right)_{ij} = \begin{bmatrix} M_{11} & M_{12} \\ M_{21} & M_{22} \end{bmatrix} \tag{3}$$

$$M_k = \begin{bmatrix} \cos\beta_k & -i\sin\beta_k/q_k \\ -iq_k\sin\beta_k & \cos\beta_k \end{bmatrix} \tag{4}$$

$$q_k = \left(\mu_k/\varepsilon_k\right)^{1/2}\cos\theta_k = \frac{\left(\varepsilon_k - n_1^2\sin^2\theta_1\right)^{1/2}}{\varepsilon_k} \tag{5}$$

Here, $\beta_k = \frac{2\pi d_k}{\lambda}\left(\varepsilon_k - n_1^2\sin^2\theta_1\right)^{1/2}$ is the arbitrary phase constant, and the angle of entrance is $\theta_k = a\cos\left(\sqrt{1 - (n_{k-1}/n_k\,)\sin^2\theta_1}\right)$ [4]. d_k is the k^{th} layer's thickness, n_k is the complex RI and ε_k is the dielectric constant of the material. $M_{11}, M_{12}, M_{21}, M_{22}$ matrix elements can be computed by using Equation (3) to Equation (5). The reflection coefficient and transmission coefficient from Fresnel's equation are expressed as follows,

$$r_p = \frac{H_y^{ref}}{H_y^{inc}} = \frac{(M_{11} + M_{12}q_N)\,q_1 - (M_{21} + M_{22}q_N)}{(M_{11} + M_{12}q_N)\,q_1 + (M_{21} + M_{22}q_N)} \tag{6}$$

$$t_p = \frac{H_{yN}{}^{\circ}}{H_y{}^{inc}} = \frac{2q_1}{(M_{11} + M_{12}q_N)\,q_1 + (M_{21} + M_{22}q_N)} \tag{7}$$

Here, H_y^{ref}, H_y^{inc} and $H_{yN}{}^{\circ}$ are the reflected, incident, and transmitted magnetic fields through the N-layer structure respectively [26]. With the increment of the analyte RI, a right shift of SPR angle occurs which can be explained by $\theta_{spr} = \sin^{-1}\frac{\eta_{eff}\,\eta_a}{\eta_p\sqrt{\eta_{eff}^2 + \eta_a^2}}$ where, η_{eff}, η_a and η_p are representing an equivalent refractive index of the composite layer, analyte, and prism respectively [56]. Condition for matching of glass WV K_x with the metal WV K_{spw} is denoted by

$$K_0 n_p\sin\theta_1 = K_0 n_a\sin\theta_t = \mathrm{Re}\left(K_0\sqrt{\frac{\varepsilon_m\varepsilon_a}{\varepsilon_m + \varepsilon_a}}\right) \tag{8}$$

Here, $k_0 = {}^{2\pi}/_{\lambda}$ is the WV in a vacuum and θ_t is the medium to prism incident angle. K_p represents the perturbation wave vector in analyte or glass prism, the total wave vector of SPW is $K = K_p + K_{spw}$ [56].

C. PERFORMANCE EVALUATING PARAMETERS

The LRSPR sensors are well suited to obtain the narrower angular width i.e., minimal full width half maxima (FWHM), higher detection accuracy (DA), and higher quality factor (QF) when compared with conventional SPR sensors [35]. Among all the major performance parameters of the SPR biosensor, the most important one is its angular sensitivity, S which is the ratio of change in resonance angle to the change in the refractive index of the sensing medium that may cause by the binding of analytes to biomolecular recognition element.

In the angular interrogation method, it is denoted by [24],

$$S = {}^{\delta\theta_{res}}/_{\delta n_s}\left({}^{\text{deg}}/_{RIU}\right) \tag{9}$$

The FWHM is defined as the difference between two predictor variable points for which the response variable is equal to half of its maximum value. QF is the ratio of angular sensitivity to FWHM [4] and is expressed as,

$$QF = \frac{S}{FWHM}\left(RIU^{-1}\right) \tag{10}$$

Detection Accuracy is the inverse to the FWHM of the reflectance intensity curve and can be denoted as [29],

$$DA = {}^{1}/_{FWHM}\left(\text{deg}^{-1}\right) \tag{11}$$

III. RESULTS AND DISCUSSION

A. THE EFFECT OF STRUCTURAL PARAMETERS

To pursue the best out of the proposed configurations, optimization of all the geometrical parameters is carried out for analyte RI ranging from 1.330 to 1.353 using TMM. There are many chemical and biological molecules that have RI within this range. For example, in a blood sample, with the increment of hemoglobin concentration, RI could vary from 1.32919 to 1.34919. The glucose level in the patient urine sample ranges from 1.336 to 1.347 for a concentration of 0.625 gm/dl to 10 gm/dl [57]. In case of chemical detection, Methanol has an RI of 1.3291, Acetonitrile has 1.3441, and Diethyl ether has 1.353 [58]. Salinity in water also varies the sample RI from 1.330 to 1.337 for concentrations from 0% to 30% [7]. To investigate the performance parameters first, we have varied the metal layer thickness from 30 to 60 nm with a step size of 5 nm to acquire the optimum trade-off between all performance parameters. Fig. 2(a) shows that both S and QF improve with the increment of thickness d_2 till 50 nm, but for the larger thickness of Ag, sensitivity reduces as the amount of light passes through this thick metal layer failed to reach the dielectric layer to form SPR. From Fig. 2(b) it can be observed that DA increases over the increment of the thickness whereas $R_{\min}$ is least in the range of 40-47 nm, and for 43 nm it is 0.068*E-4*.

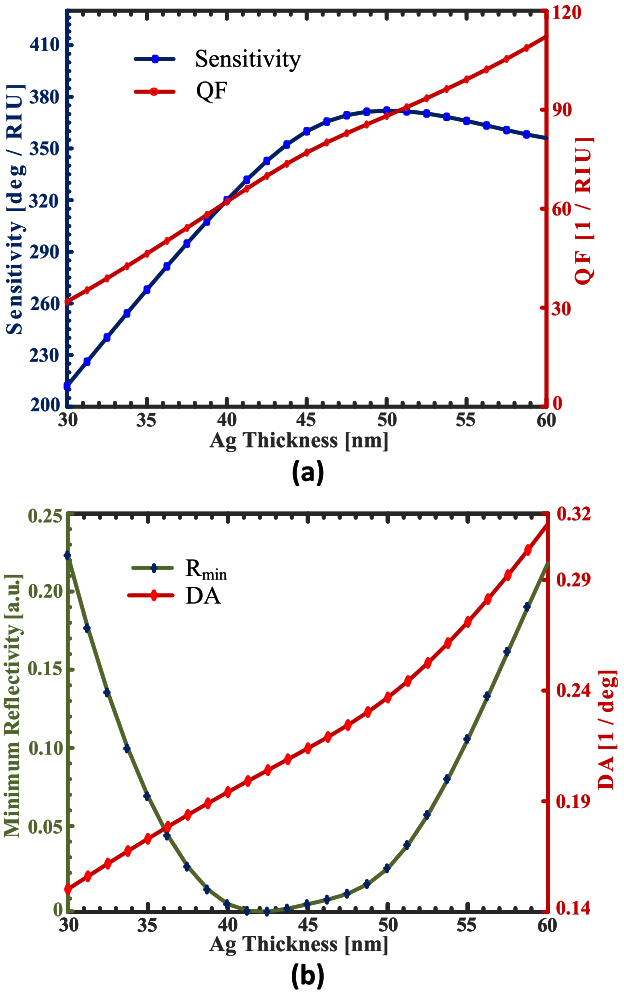

FIGURE 2. Considering config. *ii* for analyte RI 1.330 to 1.353 when d_1 = 5 nm, d_3 = 11*1 nm and d_4 = 1*2.55 nm, effect of metal layer thickness variation on (a) sensitivity and QF (b) minimum reflectivity and DA.

The thickness of the adhesive layer is needed to be as small as possible so that it has minimal effect on the device performance [22]. Fig. 3(a) shows the effect of thickness variation of Ti and Cr acting as an adhesive layer for Ag which implies a trade-off between angular S and QF is best at 5 nm for both Ti and Cr. Both of them provide similar QF characteristics whereas Ti has slightly higher angular sensitivity than Cr. Though there is a negligible difference between these two on performance, Cr is stronger than Ti which increases the overall stability of the sensor, moreover, Cr can act as a suitable passivation surface and it shows strong corrosion resistance [21]. Minimum reflectance and FWHM for thickness variation are shown in Fig. 3(b) which tells with the increment of the Cr layer thickness, FWHM decreases whereas R_{min} increases. Variation of thickness have linear effect on both parameters, where 5.0 nm is the optimal thickness for which better trade-off between R_{min} and FWHM can be achieved.

After optimizing d_1 and d_2 to 5 nm and 50 nm respectively, thickness d_3 is optimized to get the maximum performance

TABLE 3. Effect of variation of M for all configurations in terms of S, R_{min} and QF when $d_1 = 5$ nm, $d_2 = 50$ nm and analyte RI 1.330 to 1.353.

2D Material	No. of layers (M)	Sensitivity [deg/RIU]		R_{min}		QF [deg^{-1}]	
		With $BaTiO_3$	With BP	With $BaTiO_3$	With BP	With $BaTiO_3$	With BP
No 2D Layer	0	394	372	0.0228	0.0282	93.636	80.549
Graphene	1	320	310	0.1125	0.1073	67.028	60.110
	2	272	268	0.2146	0.1974	51.757	47.437
	3	228	232	0.3138	0.2871	40.135	37.902
Graphene Oxide	1	372	352	0.0228	0.0280	88.114	76.475
	2	336	320	0.0232	0.0281	82.075	71.564
	3	296	284	0.0238	0.0284	75.307	65.730
MXene	1	242	242	0.2772	0.2551	43.174	40.311
	2	78	104	0.4562	0.4270	13.095	15.962

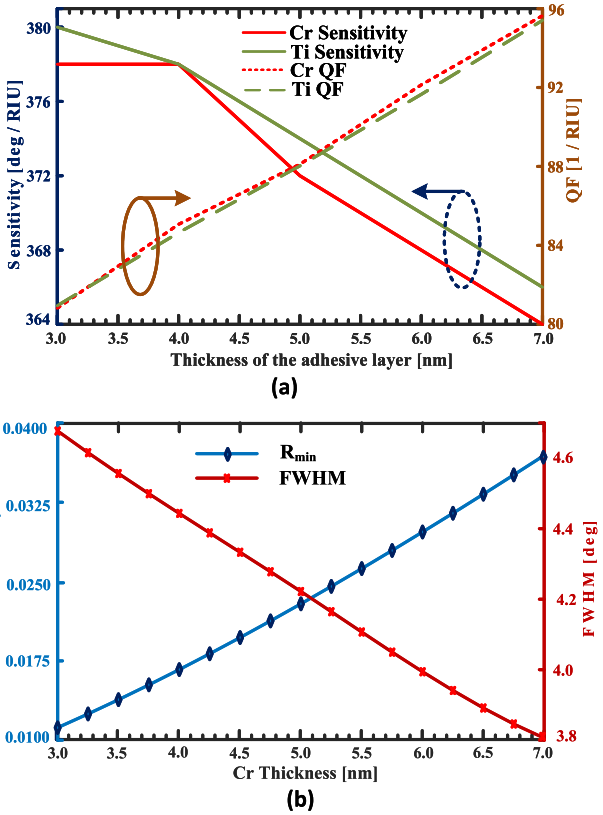

FIGURE 3. Considering config. *ii* for analyte RI 1.330 to 1.353 when $d_2 = 50$ nm, $d_3 = 11*1$ nm and $d_4 = 1*2.55$ nm, effect of adhesive layer thickness variation on (a) sensitivity and QF for Ti and Cr (b) minimum reflectivity and FWHM for Cr.

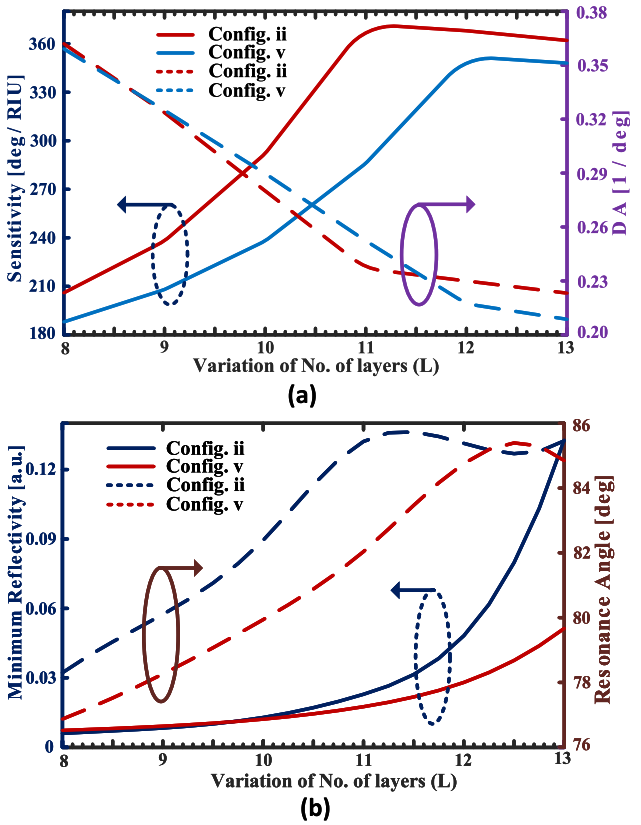

FIGURE 4. For analyte RI 1.330 to 1.353 when $d_1 = 5$ nm, $d_2 = 50$ nm and $d_4 = 1*2.55$ nm, Effect of L variation on (a) sensitivity and DA (b) minimum reflectivity and resonance angle.

from all the configurations with stable structure, the results are shown in Fig. 4. From Fig. 4(a), it is seen that comparatively, $BaTiO_3$ film provides better sensitivity than BP while having a slightly less DA for the same number of layers. A better tradeoff between these two parameters can be achieved for L = 11 (Config. *i-iii*) and L = 12 (Config. *iv-vi*) which are taken as the optimized thickness of d_3 for further optimization. Fig. 4(b) demonstrated the change of resonance angle and minimum reflectivity with the variation of L. Minimum reflectivity is quite similar for no. of layers ranging from 8 to 12 and it drastically increases for more no. of layers especially in case of $BaTiO_3$.

In addition, for refractive index 1.330 and 1.335, the reflectivity curve of all six configurations at the optimal thickness with a monolayer of 2D material is presented in Fig. 5. It clearly shows that config. *ii* and config. *v* has produced the best reflectivity curve with minimum reflectance at resonance having a larger shift of the curve concerning the variation of

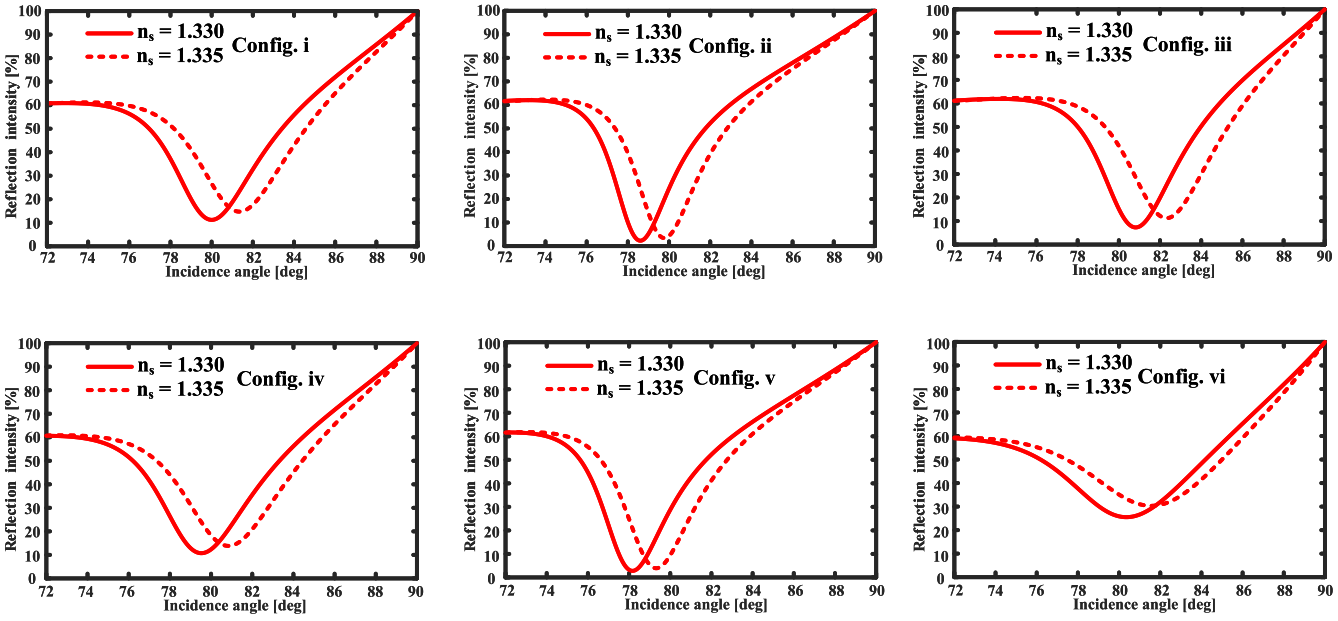

FIGURE 5. Reflectivity curve of all six configurations with monolayer of 2D materials at the optimized layer thickness for RI 1.330 and 1.335.

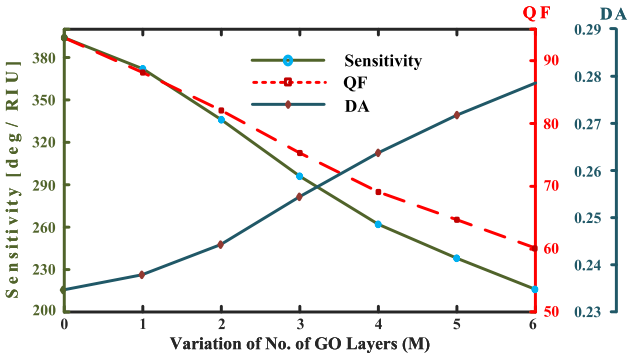

FIGURE 6. Considering config. *ii* for analyte RI 1.330 to 1.353 when d_1 = 5 nm, d_2 = 50 nm and d_3 = 11*1 nm, effect of M variation on sensitivity, QF, and DA.

the RI of the analyte. It also reflects that MXene produces a poorer reflectivity curve compared to GR and GO.

Finally, M is varied for all configurations and the result is tabulated in Table 3 where it can be observed that both sensitivity and QF are highest for M = 0 whereas they are lowest for MXene that M = 3 failed to provide right shifting reflectivity curve for config. *iii* and *vi*. It can clearly be seen that adding more numbers of layers for all configuration worsen the performance that is why M is bounded by 0 to 3 in Table 3. But, there must be a biomolecule absorber layer beneath the sensing medium, without which the sensor won't be practical to use. It can also be realized from Fig. 6 that as the number of layers increases the DA of the sensor increases but sensitivity and QF decrease. Table 3 also says that a monolayer of GO on top of the structure gives maximum sensitivity with good QF and DA to identify molecules more precisely.

The reflectivity curve of the optimized config. *ii* is plotted in Fig. 7(a) where a dip of SPR curve occurs at each RI of the analyte ranging 1.330 to 1.350 which reveal that the propose sensor can perform well for a wide range of applications. Fig. 7(b) shows the effect of the presence of 5 nm adhesive layer in the proposed sensor on the reflectivity curve. It is seen that without adhesive, the model has produced a more dipper reflectivity curve with similar sensitivity at a cost of the physical stability of the sensor at a cost of low initial dip at initial angular rotation angle.

B. TUNING THE SENSOR

It can be seen from Fig. 2 to Fig. 7 that the proposed sensor provides remarkable performance within the mentioned range but this can be further extended by reducing the number of $BaTiO_3$ layers. With tuning d_3, higher sensitivity with a better QF can be achieved for RI up to 1.410 which is reflected in Table 4. Higher the value of RI, which may be a cause of the high concentration of the biomolecules, can result in more light absorbance with a thinner layer and accomplish a larger shift in the reflectivity curve. For example, Normal MCF-7 Cells (30-70%) have an RI of 1.387 but if they are affected with Breast Cancer (80%), their RI becomes 1.401. Similarly, Normal Basal Cell (30-70%) has an RI of 1.36 whereas if they are affected with Skin Cancer (80%) their RI becomes 1.38 [23]. Moreover, 0-15 mg/dl glucose level in the patient urine sample has RI of 1.335 whereas 5 gm/dl has RI of 1.341 and it goes up to RI of 1.347 for 10 gm/dl glucose level [57]. Table 4 shows the RI of maximum sensitivity with its corresponding performance parameters. 414 deg/RIU with 119.27 deg^{-1} QF at 1.407 RI for 4 nm of $BaTiO_3$ thickness

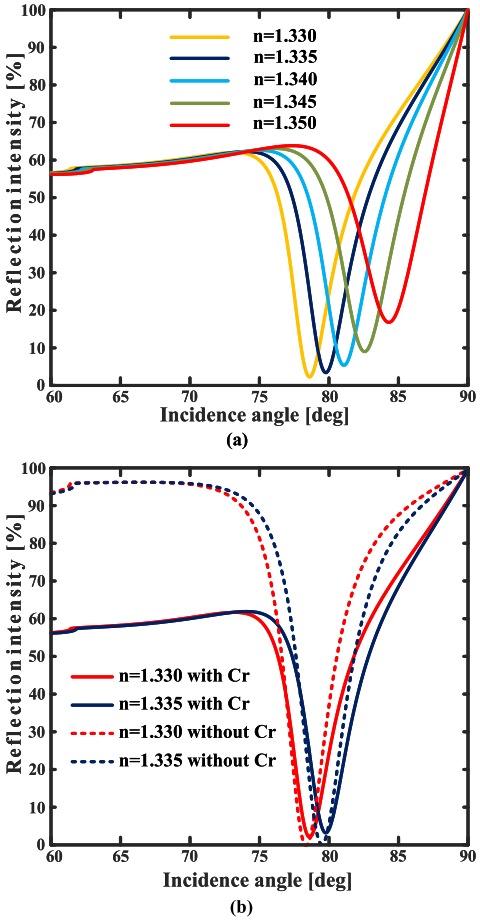

FIGURE 7. Variation of reflection intensity of the proposed sensor (a) for RI 1.330 - 1.350 (b) for RI 1.330 and 1.335 with and without the adhesive layer.

TABLE 4. Tuning sensor performance for higher RI by varying thickness of $BaTiO_3$.

$BaTiO_3$ thickness [nm]	RI	θ_{res}	R_{min}	Sensitivity [deg/RIU]	QF [deg^{-1}]
4	1.407	86.03	0.0035	414	119.272
5	1.400	85.85	0.0037	408	113.973
6	1.393	85.80	0.0040	402	109.562
7	1.386	85.87	0.0047	396	105.084
8	1.378	85.67	0.0059	390	100.804
9	1.370	85.59	0.0082	384	96.424

can be achieved in the range of analyte RI 1.330-1.410. As the thickness of $BaTiO_3$ increases, both the sensitivity, and QF decrease and resonance occur at the lower RI of the analyte.

C. ANALYSIS OF ELECTROMAGNETIC FIELD DISTRIBUTION

FEM is used to thoroughly investigate the distribution of electromagnetic field at the layer interfaces of the proposed sensor. To explore the bio-molecular interaction between reagents and analytes, it is crucial to characterize the electromagnetic field distribution since it is greatly influenced by the SPR effect. If the reflectance curve displays the lowest reflectivity value due to the SPR condition, the electromagnetic field strength is at its maximum in the field distribution curve, and vice versa. Due to the efficient charge transfer caused by the integration of the metal-dielectric layer, there is a strong coupling that significantly increases the field intensity at the sensing interface [59], [60]. This is significant because the strong electromagnetic field aids in enhancing the device's sensing and detection capabilities. Fig. 8 shows that maximum electric field at the $BaTiO_3$-GO-Sensing medium interface that apprises an enhanced interaction of light-matter. The reverse situation arises at the prism-adhesive-metal interface, due to the absence of SPR effect the field distribution dips there.

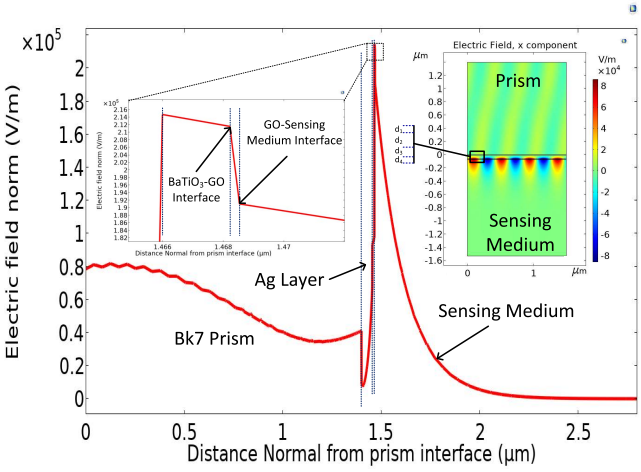

FIGURE 8. Normalized electric field distribution of the proposed configuration.

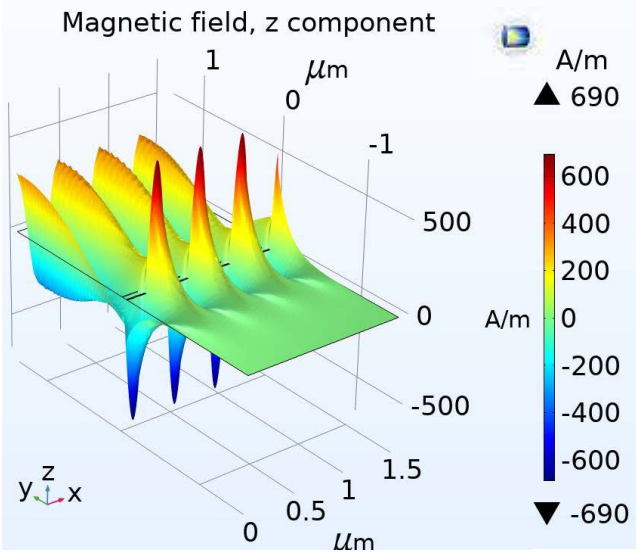

FIGURE 9. Magnetic field distribution of the proposed configuration at SPR condition.

Fig. 9 shows the propagation of the z component of the magnetic field at the resonance angle which reveals that maximum field distribution can be achieved at the SPR angle

and SPW propagates along the Ag-$BaTiO_3$ interface where the dip is found at the prism-adhesive-metal interface.

Table 5 compares the obtained performance of the proposed sensor with some previously reported models. It is observed that the designed sensor has both higher angular sensitivity and QF whereas others' works lack at obtaining a high value of both parameters at the same time. Moreover, this work has been performed at the visible range where some research was reported at NIR.

TABLE 5. Performance comparison of the proposed structure with previously reported work.

SPR Sensor Structure	Wavelength	Sensitivity [deg/RIU]	QF [deg^{-1}]	Ref
Bk7-Ag-Si-Franckeite	720	158.31	63.92	[7]
Bk7-CaF_2-ZnO-Au-BlueP-MoS_2	633	228	56.21	[15]
Bk7-Ag-$BaTiO_3$-Graphene	633	257	45.05	[24]
Bk7-Au-WSe_2-$PtSe_2$-BP	633	200	17.70	[25]
Bk7-Au-BP-Au-Graphene	633	218	26.13	[26]
Bk7-Au-WSe_2	632.8	179.32	30.65	[29]
Bk7-Au-$PtSe_2$-WS_2	633	194	17.94	[39]
Bk7-Cr-Ag-BP-GO	632.8	352	76.48	This Work
Bk7-Cr-Ag-$BaTiO_3$-GO	632.8	372	88.11	This Work

IV. CONCLUSION

A new 2D material, GO is explored at the visible range to obtain higher sensitivity and QF. Impacts of different types of materials at different layers including adhesive were investigated with varying thicknesses and the number of layers. Six different configurations were reported to achieve a maximum trade-off between the performance parameters in sample RI of 1.330 to 1.353. The proposed model provides an angular sensitivity of 372 deg/RIU with QF of 88.12 deg^{-1}, where it can be tuned for maximum sensitivity of 414 deg/RIU and QF of 119.27 deg^{-1} for higher RI up to 1.410. Fabrication of this higher precision biomolecular detector is discussed and a thin adhesive layer is used to make it suitable for practical use. It can be concluded from the extensive analysis upon the effects of layers on the sensing performance that this proposed model could pave the way for the next generation of ultrasensitive SPR-based sensors.

REFERENCES

[1] A. G. Brolo, "Plasmonics for future biosensors," *Nature Photon.*, vol. 6, no. 11, pp. 709–713, Nov. 2012.

[2] W. L. Then, M.-I. Aguilar, and G. Garnier, "Quantitative detection of weak D antigen variants in blood typing using SPR," *Sci. Rep.*, vol. 7, no. 1, pp. 1–7, Dec. 2017.

[3] Q. Wang, H. Song, A. Zhu, and F. Qiu, "A label-free and anti-interference dual-channel SPR fiber optic sensor with self-compensation for biomarker detection," *IEEE Trans. Instrum. Meas.*, vol. 70, pp. 1–7, 2021.

[4] M. S. Rahman, M. S. Anower, M. K. Rahman, M. R. Hasan, M. B. Hossain, and M. I. Haque, "Modeling of a highly sensitive MoS_2-graphene hybrid based fiber optic SPR biosensor for sensing DNA hybridization," *Optik*, vol. 140, pp. 989–997, Jul. 2017.

[5] T. Guo, "Fiber grating-assisted surface plasmon resonance for biochemical and electrochemical sensing," *J. Lightw. Technol.*, vol. 35, no. 16, pp. 3323–3333, Aug. 15, 2017.

[6] A. K. Paul, "Design and analysis of photonic crystal fiber plasmonic refractive index sensor for condition monitoring of transformer oil," *OSA Continuum*, vol. 3, no. 8, p. 2253, 2020.

[7] B. Hossain, A. K. Paul, M. A. Islam, M. F. Hossain, and M. M. Rahman, "Design and analysis of highly sensitive prism based surface plasmon resonance optical salinity sensor," *Results Opt.*, vol. 7, May 2022, Art. no. 100217.

[8] S. N. Syed Nor, N. S. Rasanang, S. Karman, W. S. W. K. Zaman, S. W. Harun, and H. Arof, "A review: Surface plasmon resonance-based biosensor for early screening of SARS-CoV2 infection," *IEEE Access*, vol. 10, pp. 1228–1244, 2022.

[9] S. S. Alabsi, A. Y. Ahmed, J. O. Dennis, M. H. M. Khir, and A. S. Algamili, "A review of carbon nanotubes field effect-based biosensors," *IEEE Access*, vol. 8, pp. 69509–69521, 2020.

[10] S. S. Alabsi, M. H. M. Khir, M. S. M. Saheed, J. O. Dennis, and A. Y. Ahmed, "Contact resistance of metal-CNT contacts in field effect based sensors," in *Proc. 8th Int. Conf. Intell. Adv. Syst. (ICIAS)*, Jul. 2021, pp. 1–4.

[11] R. Kaňok, D. Ciprian, and P. Hlubina, "Surface plasmon resonance-based sensing utilizing spatial phase modulation in an imaging interferometer," *Sensors*, vol. 20, no. 6, p. 1616, Mar. 2020.

[12] P. Suvarnaphaet and S. Pechprasarn, "Graphene-based materials for biosensors: A review," *Sensors*, vol. 17, no. 10, p. 2161, Sep. 2017.

[13] J. Homola, "Present and future of surface plasmon resonance biosensors," *Anal. Bioanal. Chem.*, vol. 377, no. 3, pp. 528–539, Oct. 2003.

[14] R. P. H. Kooyman, "Chapter 2 physics of surface plasmon resonance," in *Handbook of Surface Plasmon Resonance*. London, U.K.: Royal Society of Chemistry, 2008, pp. 15–34.

[15] S. Singh, A. K. Sharma, P. Lohia, and D. K. Dwivedi, "Theoretical analysis of sensitivity enhancement of surface plasmon resonance biosensor with zinc oxide and blue phosphorus/MoS_2 heterostructure," *Optik*, vol. 244, Oct. 2021, Art. no. 167618.

[16] C. Murphy, E. Stack, S. Krivelo, D. A. Mcpartlin, B. Byrne, C. Greef, M. J. Lochhead, G. Husar, S. Devlin, C. T. Elliott, and R. J. O. Kennedy, "Biosensors and bioelectronics detection of the cyanobacterial toxin, microcystin-LR, using a novel recombinant antibody-based optical-planar waveguide platform," *Biosensors Bioelectron.*, vol. 67, pp. 1–7, May 2014.

[17] J. Mawa Nijhum, T. Ahmed, M. A. Hossain, J. Atai, and N. H. Hai, "Microchannel-embedded D-Shaped photonic crystal fiber-based highly sensitive plasmonic biosensor," *Appl. Sci.*, vol. 12, no. 9, p. 4122, Apr. 2022.

[18] A. K. Sharma and A. K. Pandey, "Blue phosphorene/MoS_2 heterostructure based SPR sensor with enhanced sensitivity," *IEEE Photon. Technol. Lett.*, vol. 30, no. 7, pp. 595–598, Apr. 1, 2018.

[19] L. Han, X. He, L. Ge, T. Huang, H. Ding, and C. Wu, "Comprehensive study of SPR biosensor performance based on metal-ITO-graphene/TMDC hybrid multilayer," *Plasmonics*, vol. 14, no. 6, pp. 2021–2030, Dec. 2019.

[20] M. A. Mollah, S. M. A. Razzak, A. K. Paul, and M. R. Hasan, "Microstructure optical fiber based plasmonic refractive index sensor," *Sens. Bio-Sens. Res.*, vol. 24, Jun. 2019, Art. no. 100286.

[21] N. R. Mohamad, G. S. Mei, N. A. Jamil, B. Majlis, and P. S. Menon, "Influence of ultrathin chromium adhesion layer on different metal thicknesses of SPR-based sensor using FDTD," *Mater. Today, Proc.*, vol. 7, pp. 732–737, Jan. 2019.

[22] J. S. Weerakkody, S. Brenet, T. Livache, C. Herrier, Y. Hou, and A. Buhot, "Optical index prism sensitivity of surface plasmon resonance imaging in gas phase: Experiment versus theory," *J. Phys. Chem. C*, vol. 124, no. 6, pp. 3756–3767, Feb. 2020.

[23] B. Hossain, A. K. Paul, M. A. Islam, M. M. Rahman, A. K. Sarkar, and L. F. Abdulrazak, "A highly sensitive surface plasmon resonance biosensor using SnSe allotrope and heterostructure of BlueP/MoS_2 for cancerous cell detection," *Optik*, vol. 252, Feb. 2022, Art. no. 168506.

[24] P. Sun, M. Wang, L. Liu, L. Jiao, W. Du, F. Xia, M. Liu, W. Kong, L. Dong, and M. Yun, "Sensitivity enhancement of surface plasmon resonance biosensor based on graphene and barium titanate layers," *Appl. Surf. Sci.*, vol. 475, pp. 342–347, May 2019.

[25] M. M. Rahman, L. F. Abdulrazak, M. Ahsan, M. A. Based, M. M. Rana, M. S. Anower, K. A. Rikta, J. Haider, and S. Gurusamy, "2D nanomaterial-based hybrid structured (Au-WSe_2-$PtSe_2$-BP) surface plasmon resonance (SPR) sensor with improved performance," *IEEE Access*, vol. 10, pp. 689–698, 2022.

[26] Y. Singh, M. K. Paswan, and S. K. Raghuwanshi, "Sensitivity enhancement of SPR sensor with the black phosphorus and graphene with bi-layer of gold for chemical sensing," *Plasmonics*, vol. 16, no. 5, pp. 1781–1790, Oct. 2021.

[27] A. Kumar, A. K. Yadav, A. S. Kushwaha, and S. K. Srivastava, "A comparative study among WS_2, MoS_2 and graphene based surface plasmon resonance (SPR) sensor," *Sens. Actuators Rep.*, vol. 2, no. 1, Nov. 2020, Art. no. 100015.
[28] A. Kumar, A. Kumar, A. S. Kushwaha, S. K. Dubey, and S. K. Srivastava, "A comparative study of different types of sandwiched structures of SPR biosensor for sensitive detection of ssDNA," *Photon. Nanostruct., Fundam. Appl.*, vol. 48, Feb. 2022, Art. no. 100984.
[29] D. T. Nurrohman and N.-F. Chiu, "Surface plasmon resonance biosensor performance analysis on 2D material based on graphene and transition metal dichalcogenides," *ECS J. Solid State Sci. Technol.*, vol. 9, no. 11, Jan. 2020, Art. no. 115023.
[30] A. K. Pandey, "Plasmonic sensor utilizing $Ti_3C_2T_x$ MXene layer and fluoride glass substrate for bio- and gas-sensing applications: Performance evaluation," *Photon. Nanostruct., Fundam. Appl.*, vol. 42, Dec. 2020, Art. no. 100863.
[31] L. Han, H. Ding, N. N. A. Landry, M. Hua, and T. Huang, "Highly sensitive SPR sensor based on Ag-ITO-BlueP/TMDCs-graphene heterostructure," *Plasmonics*, vol. 15, no. 5, pp. 1489–1498, Oct. 2020.
[32] D. Sarid, "Long-range surface-plasma waves on very thin metal films," *Phys. Rev. Lett.*, vol. 47, no. 26, pp. 1927–1930, 1981.
[33] G. G. Nenninger, P. Tobiška, J. Homola, and S. S. Yee, "Long-range surface plasmons for high-resolution surface plasmon resonance sensors," *Sens. Actuators B, Chem.*, vol. 74, nos. 1–3, pp. 145–151, 2001.
[34] F. Pigeon, I. F. Salakhutdinov, and A. V. Tishchenko, "Identity of long-range surface plasmons along asymmetric structures and their potential for refractometric sensors," *J. Appl. Phys.*, vol. 90, no. 2, pp. 852–859, Jul. 2001.
[35] V. Chabot, Y. Miron, M. Grandbois, and P. G. Charette, "Long range surface plasmon resonance for increased sensitivity in living cell biosensing through greater probing depth," *Sens. Actuators B, Chem.*, vol. 174, pp. 94–101, Nov. 2012.
[36] A. Shalabney and I. Abdulhalim, "Sensitivity-enhancement methods for surface plasmon sensors," *Laser Photon. Rev.*, vol. 5, no. 4, pp. 571–606, 2011.
[37] A. V. Kabashin, P. Evans, S. Pastkovsky, W. Hendren, G. A. Wurtz, R. Atkinson, R. Pollard, V. A. Podolskiy, and A. V. Zayats, "Plasmonic nanorod metamaterials for biosensing," *Nature Mater.*, vol. 8, no. 11, pp. 867–871, 2009.
[38] S. Li, L. Ma, M. Zhou, Y. Li, Y. Xia, X. Fan, C. Cheng, and H. Luo, "New opportunities for emerging 2D materials in bioelectronics and biosensors," *Current Opinion Biomed. Eng.*, vol. 13, pp. 32–41, Mar. 2020.
[39] M. M. Rahman, M. M. Rana, M. S. Rahman, M. S. Anower, M. A. Mollah, and A. K. Paul, "Sensitivity enhancement of SPR biosensors employing heterostructure of $PtSe_2$ and 2D materials," *Opt. Mater.*, vol. 107, Sep. 2020, Art. no. 110123.
[40] B. Dey, M. S. Islam, and J. Park, "Numerical design of high-performance WS_2/metal/WS_2/graphene heterostructure based surface plasmon resonance refractive index sensor," *Results Phys.*, vol. 23, Apr. 2021, Art. no. 104021.
[41] L. Li, Y. Yu, G. J. Ye, Q. Ge, X. Ou, H. Wu, D. Feng, X. H. Chen, and Y. Zhang, "Black phosphorus field-effect transistors," *Nature Nanotechnol.*, vol. 9, no. 5, pp. 372–377, 2014.
[42] L. Wu, J. Guo, Q. Wang, S. Lu, X. Dai, Y. Xiang, and D. Fan, "Sensitivity enhancement by using few-layer black phosphorus-graphene/TMDCs heterostructure in surface plasmon resonance biochemical sensor," *Sens. Actuators B, Chem.*, vol. 249, pp. 542–548, 2017.
[43] J. L. Zhang, S. Zhao, C. Han, Z. Wang, S. Zhong, S. Sun, R. Guo, X. Zhou, C. D. Gu, K. D. Yuan, Z. Li, and W. Chen, "Epitaxial growth of single layer blue phosphorus: A new phase of two-dimensional phosphorus," *Nano Lett.*, vol. 16, no. 8, pp. 4903–4908, Sep. 2016.
[44] Z. Zhu and D. Tománek, "Semiconducting layered blue phosphorus: A computational study," *Phys. Rev. Lett.*, vol. 112, no. 17, pp. 1–5, May 2014.
[45] Y. Zhu, S. Murali, W. Cai, X. Li, J. W. Suk, J. R. Potts, and R. S. Ruoff, "Graphene and graphene oxide: Synthesis, properties, and applications," *Adv. Mater.*, vol. 22, no. 35, pp. 3906–3924, 2010.
[46] H. Zhang, Y. Sun, S. Gao, J. Zhang, H. Zhang, and D. Song, "A novel graphene oxide-based surface plasmon resonance biosensor for immunoassay," *Small*, vol. 9, no. 15, pp. 2537–2540, Aug. 2013.
[47] N.-F. Chiu, T.-Y. Huang, H.-C. Lai, and K.-C. Liu, "Graphene oxide-based SPR biosensor chip for immunoassay applications," *Nanosc. Res. Lett.*, vol. 9, no. 1, p. 445, Dec. 2014.
[48] A. T. Smith, A. M. LaChance, S. Zeng, B. Liu, and L. Sun, "Synthesis, properties, and applications of graphene oxide/reduced graphene oxide and their nanocomposites," *Nano Mater. Sci.*, vol. 1, no. 1, pp. 31–47, Mar. 2019.
[49] Y. Yang, S. Umrao, S. Lai, and S. Lee, "Large-area highly conductive transparent two-dimensional Ti_2CT_x film," *J. Phys. Chem. Lett.*, vol. 8, no. 4, pp. 859–865, Feb. 2017.
[50] L. Wu, Q. You, Y. Shan, S. Gan, Y. Zhao, X. Dai, and Y. Xiang, "Few-layer $Ti_3C_2T_x$ MXene: A promising surface plasmon resonance biosensing material to enhance the sensitivity," *Sens. Actuators B, Chem.*, vol. 277, pp. 210–215, Dec. 2018.
[51] X. Yuan, B. Ong, Y. Tan, D. Zhang, R. Irawan, and S. Tjin, "Sensitivity–stability-optimized surface plasmon resonance sensing with double metal layers," *J. Opt. A, Pure Appl. Opt.*, vol. 8, no. 11, p. 959, 2006.
[52] P. B. Johnson and R. W. Christy, "Optical constants of transition metals," *Phys. Rev. B, Condens. Matter*, vol. 9, no. 12, pp. 5056–5070, 1974.
[53] E. D. Palik, *Handbook of Optical Constants of Solids*, vol. 3. New York, NY, USA: Academic, 1998.
[54] N. Mao, J. Tang, L. Xie, J. Wu, B. Han, J. Lin, S. Deng, W. Ji, H. Xu, K. Liu, L. Tong, and J. Zhang, "Optical anisotropy of black phosphorus in the visible regime," *J. Amer. Chem. Soc.*, vol. 138, no. 1, pp. 300–305, 2016.
[55] T. Xue, X. Cui, J. Chen, C. Liu, Q. Wang, H. Wang, and W. Zheng, "A switch of the oxidation state of graphene oxide on a surface plasmon resonance chip," *ACS Appl. Mater. Interfaces*, vol. 5, no. 6, pp. 2096–2103, 2013.
[56] W. P. Chen and J. M. Chen, "Use of surface plasma waves for determination of the thickness and optical constants of thin metallic films," *J. Opt. Soc. Amer.*, vol. 71, no. 2, pp. 189–191, 1981.
[57] S. Mostufa, A. K. Paul, and K. Chakrabarti, "Detection of hemoglobin in blood and urine glucose level samples using a graphene-coated SPR based biosensor," *OSA Continuum*, vol. 4, no. 8, pp. 2164–2176, 2021.
[58] A. Iagatti, B. Patrizi, A. Basagni, A. Marcelli, A. Alessi, S. Zanardi, R. Fusco, M. Salvalaggio, L. Bussotti, and P. Foggi, "Photophysical properties and excited state dynamics of 4,7-dithien-2-yl-2,1,3-benzothiadiazole," *Phys. Chem. Chem. Phys.*, vol. 19, no. 21, pp. 13604–13613, 2017.
[59] A. Hoggard, L.-Y. Wang, L. Ma, Y. Fang, G. You, J. Olson, Z. Liu, W.-S. Chang, P. M. Ajayan, and S. Link, "Using the plasmon linewidth to calculate the time and efficiency of electron transfer between gold nanorods and graphene," *ACS Nano*, vol. 7, no. 12, pp. 11209–11217, Dec. 2013.
[60] A. M. Zaniewski, M. Schriver, J. Gloria Lee, M. F. Crommie, and A. Zettl, "Electronic and optical properties of metal-nanoparticle filled graphene sandwiches," *Appl. Phys. Lett.*, vol. 102, no. 2, Jan. 2013, Art. no. 023108.

MD. AREFIN ISLAM (Student Member, IEEE) was born in Brahmanbaria, Chittagong, Bangladesh, in 1998. He is currently pursuing the B.Sc. degree in electrical and electronic engineering (EEE) from the Rajshahi University of Engineering and Technology (RUET), Kazla, Rajshahi, Bangladesh.

He is also an Active Volunteer of IEEE and the Secretary of IEEE RUET Student Branch, RUET. He has authored several technical papers published by publishers, including OSA and Elsevier, in his research area. His research interests include optical biosensors, 2D materials, optical polarization filter, and low loss fiber-optic design.

ALOK KUMAR PAUL (Member, IEEE) was born in Bogura, Bangladesh, in 1993. He received the B.Sc. and M. Sc. degrees in electrical and electronic engineering (EEE) from the Rajshahi University of Engineering and Technology (RUET), Kazla, Rajshahi, Bangladesh, in 2016 and 2018, respectively.

From May 2016 to September 2016, he was a Lecturer with the Department of EEE, Varendra University, Rajshahi. From October 2016 to August 2019, he was a Lecturer with the Department of EEE, RUET, where he is currently working as an Assistant Professor. He has more than 50 (fifty) technical papers published by different publishers, including IEEE, OSA, Elsevier, and Springer, in his research area. His research interests include optical plasmonic devices, nanophotonics and plasmonics, graphene plasmonics, and interest in green technologies. He was a recipient of the EEE Association Award (the Student of the Year Award) from RUET for his outstanding academic performance while pursuing B.Sc. engineering degree and two the Best Paper Awards for two different research papers from IEEE Region 10 Humanitarian Technology Conference 2017 (IEEE R10HTC) and the 22nd International Conference on Electrical Machines and Systems (ICEMS), Harbin, China.

BELAL HOSSAIN (Member, IEEE) was born in Naogaon, Bangladesh, in 1994. He received the B.Sc. degree in electrical and electronic engineering (EEE) from the Rajshahi University of Engineering and Technology (RUET), Rajshahi, Bangladesh, in 2017, where he is currently pursuing the M.Sc. degree in optics.

Since 2019, he has been serving as a Lecturer with the Department of EEE, RUET. He has authored two journal articles and a conference paper. His research interest includes surface plasmon resonance based optical sensor for the detection of biomolecules.

AJAY KRISHNO SARKAR (Member, IEEE) was born in Rangpur, Bangladesh, in 1972. He received the B.Sc. degree in EEE from the Rajshahi University of Engineering and Technology (RUET), Rajshahi, Bangladesh, the M.Sc. degree in EEE, in Japan, and the Ph.D. degree in electronic and computer engineering from Griffith University, Australia.

He is currently working as a Professor with the Department of Electrical and Electronic Engineering (EEE), RUET. He is also a member of the Institute of Engineers Bangladesh (IEB) and he had the position in different organizing and technical committees in different international conferences at Bangladesh and abroad. He has published more than 50 technical papers in different journals and international conferences in Bangladesh and abroad. His research interests include sports and biomedical engineering, photonic crystal fiber and biosensors, microwave and RF circuits and devices, microwave absorptions, and thin films. He is also a reviewer of several journals, such as IEEE Access and *IEEE Photonics Journal*.

MD. MAHABUBUR RAHMAN was born in Narsingdi, Dhaka, Bangladesh, in 1992. He received the B.Sc. and M.Sc. degrees in electrical and electronic engineering (EEE) from the Rajshahi University of Engineering and Technology (RUET), Rajshahi, Bangladesh.

He is currently workings as an Assistant Professor with the Department of Electrical and Computer Engineering (ECE), RUET. He has authored more than 15 technical papers in journals and international conferences. His research interest includes biosensors, thin film technology, 2D materials design and characterization, optical fiber communication, and biomedical appliances.

ABU SADAT MD. SAYEM received the B.Sc. and M.Sc. degrees (Hons.) in electrical and electronic engineering from the Rajshahi University of Engineering and Technology, Bangladesh, in 2011 and 2015, respectively, and the Ph.D. degree (with the Vice-Chancellor's Commendation for Academic Excellence) in electronic engineering from Macquarie University, Australia, in 2021.

Moreover, he worked as an Assistant Professor and a Lecturer with the Department of Electrical and Electronic Engineering, Rajshahi University of Engineering and Technology. He is currently working with the School of Engineering, Macquarie University, and the School of Electrical and Data Engineering, University of Technology Sydney, Australia. His current research interests include wearable antennas, flexible antennas, transparent antennas, and antennas for biomedical applications. He regularly reviews papers for top-class journals in his research field. He was a recipient of several prestigious awards and scholarships, including the Vice-Chancellor's Commendation on Ph.D. Thesis, the Commonwealth Government funded International Research Training Program Scholarship to support the Ph.D. in Australia, the Prime Minister Gold Medal from Bangladesh, and the University Gold Medal from the Rajshahi University of Engineering and Technology.

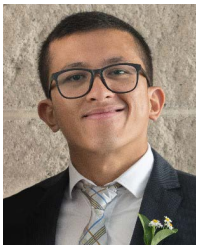

ROY B. V. B. SIMORANGKIR (Member, IEEE) received the B.S. degree in telecommunication engineering from the Bandung Institute of Technology, Indonesia, in 2010, the M.S. degree in electrical and electronic engineering from Yonsei University, South Korea, in 2014, and the Ph.D. degree in electronic engineering from Macquarie University, Australia, in 2018.

He is currently with the Wireless Sensor Network Group, Tyndall National Institute, Ireland, as a Senior Postdoctoral Researcher. He has over 50 refereed publications in this area. His general research interests include development of flexible/stretchable antennas and sensors utilizing unconventional materials.

Dr. Simorangkir was a recipient of a number of major awards. He was awarded the Highly Competitive Korean Government Scholarship Program for his master's degree, from 2012 to 2014. During his Ph.D., he succeeded the International Macquarie University Research Excellence Scholarship (iMQRES), from 2015 to 2018; the Macquarie University Postgraduate Research Fund (PGRF) with the Deputy Vice-Chancellor Commendation, in 2017; and the Wireless Medical (WiMed) Research Centre Travel and Project Grants, from 2015 to 2017. In 2017, he was a part of the team who won the Macquarie Student Startup Pitch Competition and the Commonwealth Scientific and Industrial Research Organization (CSIRO)-sponsored ON PRIME 2 pre-accelerator fund for research commercialization. In the same year, one of his works received the First Prize in the IEEE Region 10 (Asia-Pacific) Best Student Paper Contest (postgraduate category) and was a finalist in the Student Paper and Advanced Practice Paper Competitions of the IEEE MTT-S International Microwave Symposium (IMS), Honolulu. He was recently granted the prestigious 2022 Government of Ireland Fellowship to further his research on fully printed multimode adaptive antennas. He is also serving as the Guest Editor of Special Issues for *Sensors* (MDPI) and *Electronics* (MDPI). He was the Special Session Co-Chair in the 2018 International Applied Computational Electromagnetics Society (ACES) Symposium, Beijing; the 2021 Asia-Pacific Microwave Conference (APMC), Adelaide; and the 2021 IEEE International Symposium on Antennas and Propagation (AP-S), Singapore. He was the Publicity Chair of the 2022 International Workshop on Antenna Technology (iWAT), Dublin. He has been a frequent reviewer for several reputable journals in his research field. He was acknowledged as an Outstanding Reviewer of the IEEE Transaction on Antennas and Propagation for two consecutive years, in 2021 and 2022.

MD ASADUZZAMAN SHOBUG (Graduate Student Member, IEEE) was born in Sirajganj, Bangladesh, in 1991. He received the bachelor's and master's degrees in electrical and electronic engineering from the Rajshahi University of Engineering and Technology, Rajshahi, Bangladesh, in 2013 and 2019, respectively.

He has been working as a Faculty Member with the Department of Electrical and Electronic Engineering, Pabna University of Science and Technology, Pabna, Bangladesh, since 2014. He successfully completed his tenure as a Advisor for the IEEE PUST Student Branch, from 2020 to 2021. His research interest includes optical biosensors, renewable wind energy, and smart grid.

JOHN L. BUCKLEY (Member, IEEE) received the B.Eng. degree from the Cork Institute of Technology (CIT), 1994, and the M.Eng.Sc. and Ph.D. degrees from the University College Cork (UCC), Ireland, in 2004 and 2016, respectively. He was with EMC Corporation, Cork, Ireland, from 1994 to 2002 where he specialized in PCB design, high-speed digital design, and signal integrity. He joined the Tyndall National Institute, University College Cork, in 2005, where he is currently a Senior Researcher and leads the Antenna and RF Team's research activities working on both fundamental and applied antenna and RF research. He has published more than 50 scientific works and acts as reviewer for several international antenna journals and conferences. He has a long track record of developing antenna and RF technologies for industry. His research interests include electrically small antenna design, tunable antennas, wearable and implantable antennas, and RF front-end design. He was a recipient of commercialization awards for technologies licensed to industry.

KISALAYA CHAKRABARTI (Senior Member, IEEE) received the Ph.D. degree from the University of Tsukuba, Japan. He has 21 years of teaching and research experience in the field of electronics and communication engineering.

He has administrative experiences as the Chair Professor with the Department of Electronics and Communication Engineering, Bengal Institute of Technology and Management, Santiniketan, where he has also worked as the Dean (Research and Development) for few months. He is currently working as a Professor with the Department of Electronics and Communication Engineering, Haldia Institute of Technology, Haldia, Purba Medinipur, India. He has been the Life Fellow of The Optical Society of India, since 2005. His research interest includes optical communications. He has two Postdoctoral Certificates from Utsunomiya University and the National Institute for Material Science, Japan. He was the recipient of prestigious Monbukagakusho (MEXT) Scholarship for his doctoral program at the University of Tsukuba from the Japanese Government.

ALI LALBAKHSH (Senior Member, IEEE) received the B.S. and M.S. degrees in electronic and telecommunication engineering, in 2008 and 2011, respectively, and the Master of Research (H.D.) and Ph.D. degrees in electronics engineering from Macquarie University, Australia, in 2015 and 2020, respectively. He holds an academic position (Macquarie University Research Fellowship) with Macquarie University. He has published over 80 peer-reviewed journal and conference papers. His research interests include satellite communication, high-gain antennas, evolutionary optimization methods, and passive microwave components. He received several prestigious awards, including the International Research Training Program Scholarship (iRTP) for MRes, the International Macquarie University Research Excellence Scholarship (iMQRES) for the Ph.D. degree, the Commonwealth Scientific and Industrial Research Organization (CSIRO) Grants on Astronomy and Space Exploration, the Macquarie University Postgraduate Research Fund (PGRF), and the WiMed Travel Support Grants. He was a recipient of the 2016 ICEAA-IEEE APWC Cash Prize and the Macquarie University Deputy Vice-Chancellor Commendation, in 2017. He was awarded the Third Prize, in 2016; the First Prize, in 2018; and the Second Prize, in 2019, from the International Competition. He is the only Researcher in the IEEE Region Ten (Asia-Pacific), who received the Most Prestigious Best Paper Contest of the IEEE Region Ten more than once. He is the highly commended finalist and the winner of the Excellence in Higher Degree Research Award in Science, Technology, Engineering, Mathematics, and Medicine (STEMM), Macquarie University, in 2019 and 2020, respectively. He has received the Research Excellence Award of the Faculty of Science and Engineering, Macquarie University. In 2020, he was announced as an Outstanding Reviewer of IEEE TRANSACTIONS ON ANTENNAS AND PROPAGATION. He serves as an Associate Editor for the *International Journal of Electronics and Communications* (AEU) and *Electronics* (MDPI).